Safe Joint Mechanism based on Passive Compliance for Collision Safety

Jung-Jun Park[1], Jae-Bok Song[1*], and Hong-Seok Kim[2]
[1]*Dept. of Mechanical Eng., Korea University, Seoul, Korea*
[2] *Center for Intelligent Robot, Korea Institute of Industrial Technology, Ansan, Korea*
* Corresponding Author: jbsong@korea.ac.kr

***Abstract*-A safe robot arm can be achieved by either a passive or active compliance system. A passive compliance system composed of purely mechanical elements often provide faster and more reliable responses for dynamic collision than an active one involving sensors and actuators. Since both positioning accuracy and collision safety are important, a robot arm should exhibit very low stiffness when subjected to a collision force greater than the one causing human injury, but maintain very high stiffness otherwise. To implement these requirements, a novel safe joint mechanism (SJM), which consists of linear springs and a slider-crank mechanism, is proposed in this research. The SJM has the advantages of variable stiffness which can be achieved only by passive mechanical elements. Various experiments of static and dynamic collisions showed the high stiffness of the SJM against an external force of less than the critical impact force, but an abrupt drop in the stiffness when the external force exceeds the critical force, thus guaranteeing collision safety. Furthermore, the critical impact force can be set to any value depending on the application.**

I. INTRODUCTION

For industrial robots, safe human-robot coexistence is not as important as the fast and precise manipulation. However, service robots often interact directly with humans for various tasks. For this reason, safety has become one of the most important issues in service robotics. Therefore, several types of compliant joints and flexible links of a manipulator have been proposed for safety.

A safe robot arm can be achieved by either a passive or active compliance system. In the actively compliant arm, collision is detected by various types of sensors, and the stiffness of the arm is properly controlled. The active compliance-based approach suffers from the relatively low bandwidth because it involves sensing and actuation in a response to dynamic collision. This rather slow response can be improved slightly when non-contact sensors such as proximate sensors are employed. Furthermore, the installation of the sensor and actuator in the robot arm often leads to high cost, an increase in system size and weight, possible sensor noise, and actuator malfunction.

On the other hand, the robot arm based on passive compliance is usually composed of the mechanical components such as a spring and a damper, which absorb the excessive collision force. Since this approach does not utilize any sensor or actuator, it can provide fast and reliable responses even for dynamic collision. Various safety mechanisms based on passive compliance have been suggested so far. The programmable passive impedance component using an antagonistic nonlinear spring and a binary damper was proposed to mimic the human muscles [1]. The mechanical impedance adjuster with a variable spring and an electromagnetic brake was developed [2]. The programmable, passive compliance-based shoulder mechanism using an elastic link was proposed [3]. A passive compliance joint with rotary springs and a MR damper was suggested for the safe arm of a service robot [4]. A variable stiffness actuator with the nonlinear torque transmitting system composed of a spring and a belt was developed [5].

Most passive compliance-based devices use linear springs. However, one drawback to the use of a linear spring is positioning inaccuracy due to the continual operation of the spring even for small external forces that do not require any shock absorption and due to undesirable oscillations caused by the elastic behavior of the spring. To cope with this problem, some systems adopt the active compliance approach by incorporating extra sensors and actuators such as electric dampers or brakes, which significantly impair the advantages of a passive system. In this research, therefore, a novel passive compliance-based safety mechanism that can overcome the above problems is proposed.

Some tradeoffs are required between positioning accuracy and safety in the design of a manipulator because high stiffness is beneficial to positioning accuracy whereas low stiffness is advantageous to collision safety performance. Therefore, the manipulator should exhibit very low stiffness when subjected to collision force greater than the one that causes injury to humans, but should maintain very high stiffness otherwise. Of course, this ideal feature can be achieved by the active compliance approach, but this approach often causes the several shortcomings mentioned above.

In the previous research, this ideal feature was realized by a novel design of the safe link mechanism (SLM) which was based on the passive compliance [6]. However, a safe mechanism, which is simpler and more lightweight than SLM, is desirable for a service robot arm. To implement these requirements, the safe joint mechanism (SJM) which possesses the same characteristics as SLM is proposed in this research. The SJM is composed of the passive mechanical elements such as linear springs and a slider-crank mechanism. The springs are used to absorb the high collision force for safety, while the slider-crank mechanism determines the safety or non-safety of the external force so that the SJM operates only in case of an emergency. The main contribution of this proposed device is the variable stiffness capability

implemented only by use of passive mechanical elements. Without compromising positioning accuracy for safety, both features can be achieved simultaneously with the SJM.

The rest of the paper is organized as follows. The operating principle of the SJM is discussed in detail in section II. Section III presents further explanation about its operation based on simulations. Various experimental results for both static and dynamic collisions are provided in section IV. Finally, section V presents conclusions and future work.

II. Operating Principle of Safe Joint Mechanism

The passive safety mechanism proposed in this research is composed of a spring and a slider-crank mechanism. This chapter presents the concept of the transmission angle of the slider-crank mechanism and the characteristics of the slider-crank mechanism in combination with the spring.

Springs have been widely used for a variety of safety mechanisms because of their excellent shock absorbing property. Since the displacement of a linear spring is proportional to the external force, the robot arm exhibits deflection due to its own weight and/or payloads when a spring is installed at the manipulator joint. This characteristic is beneficial to a safe robot arm, but has an adverse effect on positioning accuracy. To cope with this problem, it is desirable to develop a spring whose stiffness remains very high when an external force acting on the end-effector is within the range of the normal operation, but becomes very low when it exceeds a certain level of force due to collision with the object. However, no such springs with this ideal feature exist. In this research, the power transmission characteristics of the 4-bar linkage are exploited to achieve this nonlinear spring feature.

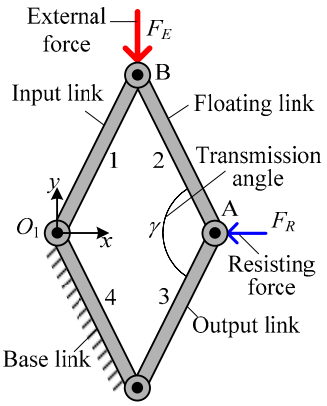

Fig. 1 4-bar linkage.

Consider a 4-bar linkage mechanism shown in Fig. 1. When an external force F_E is exerted on point B of the input link in the y-axis direction, an appropriate resisting force F_R acting in the x-axis direction can prevent the movement of the output link. In the 4-bar linkage, the transmission angle is defined as the angle between the floating and the output link. The power transmission efficiency from input to output varies depending on this transmission angle. If the transmission angle γ is less than 45° or greater than 135°, a large force is required at the input link to move the output link. That is, only a small F_R is sufficient to prevent the output link from moving for a given F_E in this case. However, as the transmission angle approaches 90°, the power transmission efficiency improves, thus leading to easy movement of the output link of a 4-bar linkage [7] Therefore, a large F_R is required to prevent the output link from moving for a given F_E.

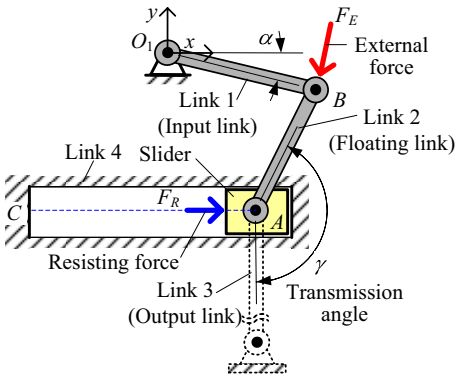

Fig. 2 Slider-crank mechanism.

The slider-crank linkage can be regarded as the 4-bar linkage if the slider is replaced by an infinitely long link perpendicular to the sliding path as shown Fig. 2. Therefore, revolute joint A between link 2 and link 3 can move rectilinearly only in the x-axis direction. Note that the transmission angle of a slider-crank mechanism can be also defined as the angle between the floating link (link 2) and the output link (link 3). The force balance of the forces acting on the slider and the input link can be given by

$$F_R = -F_E \frac{\sin\gamma}{\cos(\gamma+\alpha)} \tag{1}$$

where α is the inclined angle of link 1. Note that the value of $\sin\gamma/\cos(\gamma+\alpha)$ is always negative because γ is in the range of 90° to 180° in Fig. 2, which requires the minus sign in Eq. (1). In Eq. (1), for the same external force, the resisting force changes as a function of γ.

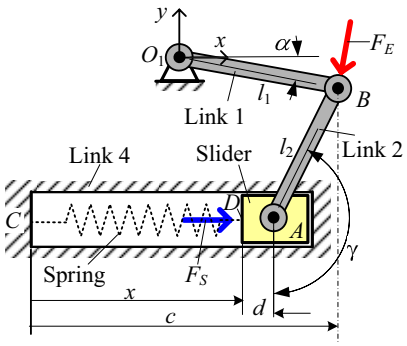

Fig. 3 Slider-crank mechanism combined with spring.

If the pre-compressed spring is installed between points C and D in Fig. 3, the spring force F_S can offer the resisting force F_R, which resists the movement of the slider caused by the external force F_E. When the external force is balanced

against the spring force, the external force can be described in terms of the transmission angle and the other geometric parameters as follows:

$$F_E = -k(s_o - c + d + l_2 \sin\gamma)\frac{\cos(\gamma+\alpha)}{\sin\gamma} \quad (2)$$

where k is the spring constant, s_o the initial length of the spring, l_2 the length of link 2 and x the displacement of the slider. Although x does not explicitly appear in Eq. (2), it is directly related to γ by the relation of $x = c - d - l_2\cos(\gamma - 90^o)$. For example, when k = 0.8kN/m, $l_1 = l_2$ = 19mm, s_0 = 34mm, c = 36mm, d = 6.5mm and α = 20°, the external force for the static force balance can be plotted as a function of γ in Fig. 4. The spring force does not need to be specified for static balance because it is automatically determined for a given γ. As shown in the figure, the external force diverges rapidly to positive infinity as γ approaches 180°, so even a very small spring force can make this mechanism statically balanced against a very large external force. In this research, the transmission angle in the range of 150° to 170° is mainly used in consideration of the mechanical strength of the mechanism.

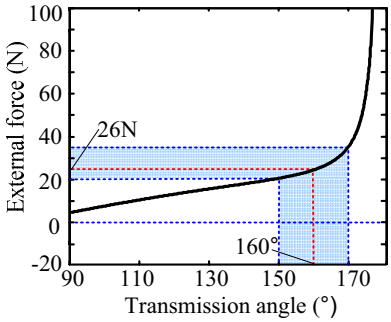

Fig. 4 External force as a function of transmission angle.

In this proposed mechanism, the external force required to balance with the spring force is defined as the *critical impact force*. For a given γ, a static balance is maintained when the external force equals the critical impact force, as shown in Fig. 4, but the spring is rapidly compressed once the external force greater than this critical value acts on this mechanism. The detailed explanation about this phenomenon is given below.

Figure 5 shows the resisting force curves for the three given external forces (F_E = 1, 26, 60N) as a function of the transmission angle γ, which is computed by Eq. (1). The spring force as a function of γ is also plotted in Fig. 5. Note that the variation of the spring force is much smaller than that of the resisting force throughout the wide range of γ. Since the spring force provides the resisting force, when the two forces are equal, the mechanism becomes statically balanced, as shown in Fig. 3.

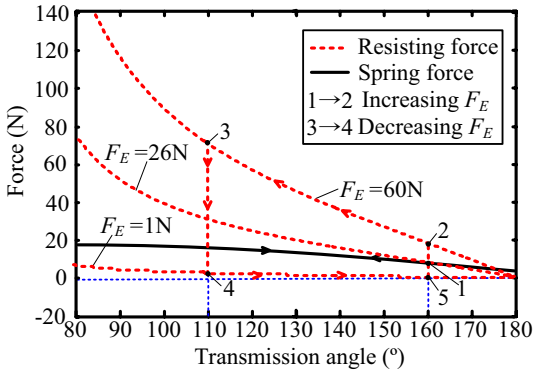

Fig. 5 Plots of resisting force and spring force versus transmission angle for high and low critical impact forces.

Suppose the critical impact force is set to 26N. Then the transmission angle γ for the static equilibrium becomes 160° from Eq. (2) with F_E = 26N. This corresponds to equilibrium point 1, which is the intersection of the resisting force curve of F_E = 26N and the spring force curve. Now suppose the external force abruptly increases to 60N, which is larger than the critical impact force (1→2), then γ reduces as the slider moves to the left in Fig. 3. As γ decreases, the resisting force rapidly increases (2→3), and the spring force also slightly increases, as shown in Fig. 5. Since the resisting force required for the static equilibrium becomes much larger than the spring force, the static equilibrium cannot be maintained, and thus the slider moves left rapidly. When the external force is reduced to 1N which is less than the critical impact force (3→4), the spring force becomes larger than the resisting force required and γ increases because the slider is pushed right (4→5) by the spring force.

III. SAFE JOINT MECHANISM MODEL

A. Prototype modeling

The mechanisms introduced conceptually in the previous section are now integrated into the safe joint mechanism (SJM), which suggests a new concept of a safe robot arm. The SJM consists of a slider-crank mechanism and a linear spring. As shown in Fig. 6, the slider-crank mechanism is installed at the fixed plate and the robot link is connected to the rotating plate. The rotation centers of both plates are identical and the collision force can be transmitted to the slider-crank mechanism by means of the force transmission shaft fixed at the rotating plate. The slider-crank mechanisms are arranged symmetrically so that they can absorb the collision force applied in both directions.

In this prototype, the collision force acting on the end-effector is amplified according to the ratio of the rotation radius of the force transmission shaft to that of the end-effector, and is transmitted to point B of the input link by the force transmission shaft. Therefore, the external force exerted on the SJM is proportional to the collision force.

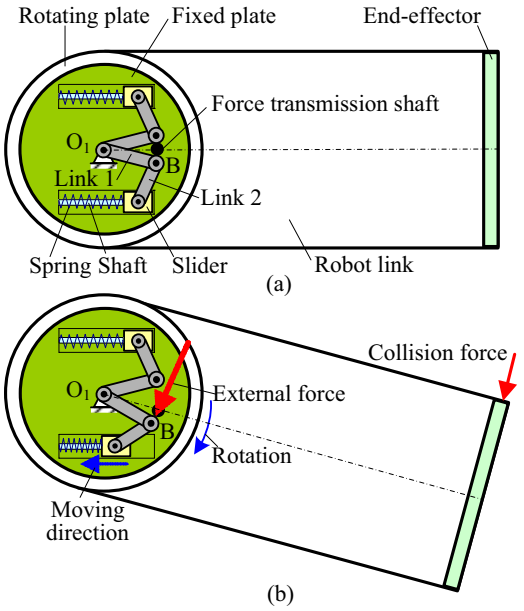

Fig. 6 Operation of SJM; (a) before collision, and (b) after collision.

If the external force exceeding the critical impact force is applied to the input link of the slider-crank mechanism by the force transmission shaft connected to the rotating plate, then the input link is rotated around point O_1, as shown in Fig. 6(b). Then, the slider connected to link 2 is forced to move left on the guide shaft to compress the spring. This movement of the slider reduces the transmission angle, so maintaining the static balance requires a greater resisting force for the same external force. However, the increased spring force due to its compression is not large enough to sustain the balance. This unbalanced state causes the slider to rapidly slide left. As a result, the force transmission shaft fixed at the rotating plate is rotated and the robot link is also rotated, which absorbs the collision force. However, if the external force amplified from the collision force is less than the critical impact force, the end-effector does not move at all, and the slider-crank mechanisms maintain the static equilibrium, thus providing high stiffness to the SJM.

B. Simulations of Prototype

Various simulations were conducted to evaluate the performance of the proposed SJM. As shown in Fig. 7, the components of the mechanism were modeled by Solidworks and its dynamics was analyzed by Visual Nastran 4D. For simplicity of simulation, only one slider-crank mechanism of the SJM was modeled by assuming that the external force directly acted on the end-effector of the robot link. The slider moving on the guide shaft was modeled as a spring-damper system. The damper was modeled to represent the friction between the slider and the shaft, although a damper was not used for the real system.

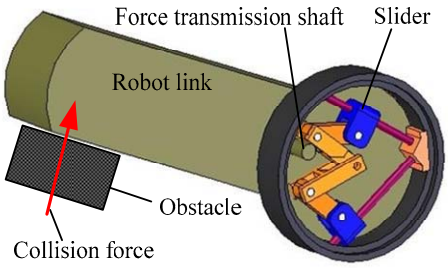

Fig. 7 Modeling of safety mechanism.

Figure 8 shows the simulation results for a static collision. As the external force acting on the end-effector increases linearly up to 60N during 1sec, the transmission angle is drastically changed, as shown in Fig. 8(b). In this simulation, the damping coefficient is set to c=1kg/s, the spring constant to k=8kN/m and the initial transmission angle to 160°. As shown in Fig. 8(b), the transmission angle does not change for the external force less than the critical impact force (in this simulation, 31N). However, once the external force exceeds this critical impact force, the transmission angle sharply decreases. In summary, the SJM stiffness remains very high like a rigid joint while the external force is below 31N. In the range of 31 to 33N, the transmission angle and thus the stiffness decrease. As the collision force approaches 33N, the stiffness abruptly diminishes, and consequently, the SJM behaves as a compliant joint.

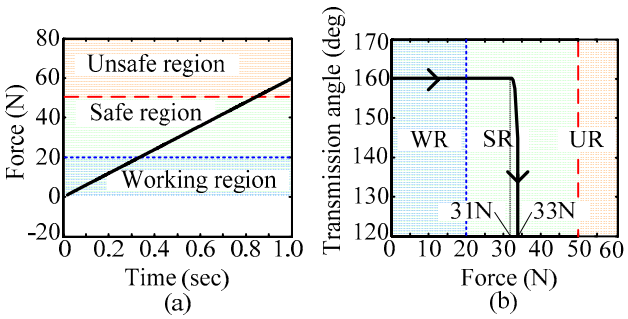

Fig. 8 Simulation results for static collision for initial transmission angle of 160°; (a) external force versus time, and (b) transmission angle versus external force.

IV. Experiments for Safe Joint Mechanism

A. Prototype of SJM

The prototype of the SJM shown in Fig. 9 was constructed to conduct various experiments related to the performance of the SJM. Most components are made of duralumin and polyoxymethylene which can endure the shock exerted on the SJM. The slider can slide and the spring can be compressed by means of the linear bushing guides.

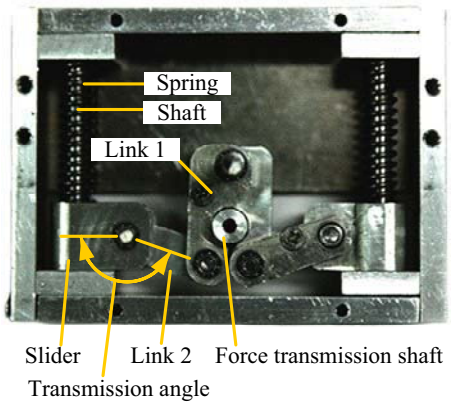

Fig. 9 Prototype of SJM.

B. Safety criterion

The safety criterion can be divided into static and dynamic collisions. The static collision means that the collision speed of the robot arm relative to a human is very low (e.g., below 0.6m/s). The human pain tolerance for static collision can be expressed by

$$F \le F_{\text{limit}} \tag{6}$$

where F_{limit} is the injury criterion value which has been suggested as 50N by several experimental researches [8].

In the case of dynamic collision, both the collision force and the collision speed are important. To represent human safety associated with the dynamic collision of the SJM, the head injury criterion (HIC), which is used to quantitatively measure head injury risk in car crash situations, is adopted in this research [9].

$$HIC = T\left(\frac{1}{T}\int_0^T a(t)\,dt\right)^{2.5} \tag{7}$$

where T is the final time of impact and $a(t)$ is the acceleration in the unit of gravitational acceleration g. An HIC value of 1,000 or greater is typically associated with extremely severe head injury, and a value of 100 can be considered suitable to normal operation of a machine physically interacting with humans.

C. Experimental results

Figure 10 shows an experimental setup in which the SJM is installed at the 1-DOF robot arm. The fixed plate of the SJM in Fig. 6 is attached to the motor and the force transmitting shaft is connected to the robot arm. Therefore, the torque of a motor can be transmitted to the robot link via the SJM. A force/torque sensor is installed at the end of the wall to measure the collision force. The displacement of the SJM is measured by an encoder attached to the SJM.

In the experiment for static collision, the spring constant was 8kN and the initial transmission angle was set to 160°. The end-effector of the robot arm was initially placed to barely touch a fixed wall, and its joint torque provided by the motor was increased slowly. The static collision force between the robot link and the wall was measured by the 6 axis force/torque sensor. Experiments were conducted for the robotic arms with and without the SJM.

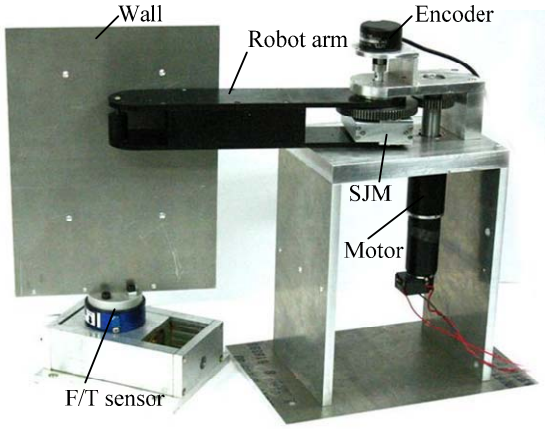

Fig. 10 Experimental setup for robot arm with SJM.

The robot arm without the SJM delivered a contact force that increased up to 70N to the wall, as shown in Fig. 11(a). However, the contact force of only up to 38N was transmitted to the wall for the robot arm with the SJM, as shown in Fig. 11(a). In other words, the contact force above the pain tolerance does not occur because the excessive force is absorbed by the SJM. In Fig. 11(b), virtually no angular displacement of the SJM attached to the robot arm occurs when the contact force is below the critical impact force of 26N. Therefore, the robot arm with the SJM can accurately handle a payload up to approximately 2kg as if it were a very rigid joint. As the contact force rises above the critical impact force, the SJM stiffness quickly diminishes and the angular displacement occurs, thus maintaining the robot arm in the safe region. In summary, the SJM provides high positioning accuracy of the robot arm in the working region, and guarantees safe human-robot contact by absorbing the contact force above 50N in the unsafe region.

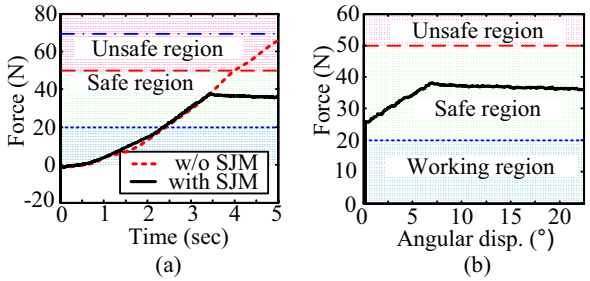

Fig. 11 Experimental results for static collision for robot arm; (a) collision force versus time without and with SJM, and (b) collision force versus angular displacement of SJM.

Next, some experiments on dynamic collision were conducted for the robot arm equipped with the SJM. The

experimental conditions including the spring constant and the initial transmission angle were set to the same values as those of static collision experiments. For dynamic collision, a plastic ball of 1.5kg moving at a velocity of 3m/s was forced to collide with the end-effector of the robot arm. The acceleration of the ball was measured by the accelerometer mounted at the ball.

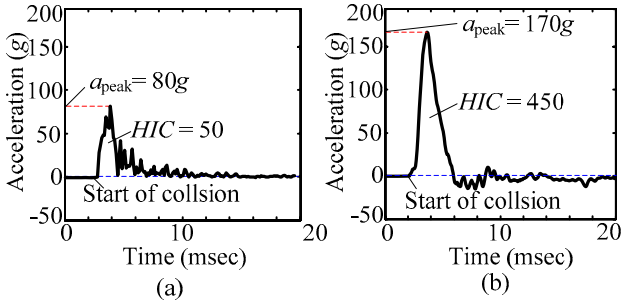

Fig. 12 Experimental results for dynamic collision of robot arm; acceleration versus time (a) with SJM, and (b) without SJM.

The experimental results are shown in Fig. 12. At the instant the ball contacts the end-effector, the acceleration of the ball reached a peak value of 80*g*, but immediately after collision, the collision force delivered to the ball dropped rapidly because of the operation of the SJM. The dynamic collision safety of the robot arm with the SJM can be verified in terms of HIC defined by Eq. (7). The HIC value was computed as 50, which is far less than 100. Therefore, the safe human-robot contact can be achieved even for this harsh dynamic collision.

Figure 12(b) shows the experimental results for the dynamic collision of the robot arm without the SJM. The peak value of the acceleration is almost twice that of the robot arm with the SJM, and the HIC value reached as high as 450, which indicates a high risk of injury to a human. Therefore, the robot arm with the SJM provides much greater safety for human-robot contact than that without the SJM.

V. Conclusions

In this research, the safe joint mechanism (SJM) was proposed. The SJM maintains very high stiffness up to the pre-determined critical impact force, but provides very low stiffness above this critical value, at which point the SJM absorbs the impact acting on the robot arm. From the analysis and experiments, the following conclusions are drawn:

1) The SJM has very high stiffness like a rigid joint when the external force acting on it is less than the critical impact force. Therefore, high positioning accuracy of the robot arm can be achieved in normal operation.

2) When the external force exceeds the critical impact force, the stiffness of the SJM abruptly drops. As a result, the robot arm acts as a compliant joint with high compliance. Therefore, human-robot collision safety can be attained even for a high-speed dynamic collision.

3) The critical impact force of the SJM can be set accurately by adjusting the initial transmission angle of the slider-crank mechanism, the spring constant and the initial spring length.

4) The proposed SJM is based on passive compliance, so it shows faster response and higher reliability than that based on the active compliance having sensors and actuators.

Currently, to apply the SJMs to two or more joints of the robot arm, the simpler and lightweight model is under development.

Acknowledgement

This research was supported by the Personal Robot Development Project funded by the Ministry of Commerce, Industry and Energy of Korea.

References

[1] K. F. Laurin-Kovitz and J. E. Colgate, "Design of components for programmable passive impedance", *Proc. of the IEEE International Conference on Robotics and Automation*, pp.1476-1481, 1991.

[2] T. Morita and S. Sugano, "Development of one-D.O.F. robot arm equipped with mechanical impedance adjuster", *Proc. of the IEEE/RSJ International Conference on Intelligent Robots and System*, pp. 407-412, 1995.

[3] M. Okada, Y. Nakamura and S. Ban, "Design of programmable passive compliance shoulder mechanism", *Proc. of the IEEE International Conference on Robotics and Automation*, pp.348-353, 2001.

[4] S. Kang and M. Kim, "Safe Arm Design for Service Robot", *Proc. of the International Conference on Control, Automation and System*, pp.88-95, 2002.

[5] G. Tonietti, R. Schiavi and A. Bicchi, "Design and Control of a Variable Stiffness Actuator for Safe and Fast Physical Human/Robot Interaction", *Proc. of the IEEE International Conference on Robotics and Automation*, pp. 528-533, 2005.

[6] J. Park, B. Kim and J. Song, "Safe Link Mechanism based on Passive Compliance for Safe Human-Robot Collision", *Proc. of the IEEE International Conference on Robotics and Automation*, 2007, to be published.

[7] C. E. Wilson and J. P. Sadler, *Kinematics and Dynamics of Machinery*, 2nd Edition, HaperCollins, 1993, pp. 30-33.

[8] Y. Yamada, Y. Hirasawa, S.Y. Huang and Y. Umetani, "Fail-safe human/robot contact in the safety space", *IEEE International Workshop on Robot and Human Communication*, pp. 59-64, 1996.

[9] J. Versace, "A review of the severity index", *Proc. of the 15th Stapp Car Crash Conference*, pp.771–796, 1971.